Measurements of fluence profiles in femtosecond laser sparks and superfilaments in air

Zhanna Samsonova,[1] Daniil Kartashov,[1] Christian Spielmann,[1] Sergey Bodrov,[2] Aleksey Murzanev,[2] Vytautas Jukna,[3,4]
Massimo Petrarca,[5] Arnaud Couairon,[4] and Pavel Polynkin[6,*]

[1]*Institute of Optics and Quantum Electronics, Abbe Center of Photonics, Friedrich-Schiller University Jena,*
Max-Wien-Platz 1, Jena 07743, Germany
[2]*Institute of Applied Physics, Russian Academy of Sciences, 46 Ulyanov St., Nizhny Novgorod 603950, Russia*
[3]*Laser Research Center, Vilnius University, Saulėtekio Ave. 10, LT-10223 Vilnius, Lithuania*
[4]*Centre de Physique Théorique, Ecole Polytechnique, CNRS, Université Paris-Saclay, Route de Saclay, F-91128 Palaiseau, France*
[5]*La Sapienza University, SBAI Department, via A. Scarpa 14, 00161 Rome, Italy*
[6]*College of Optical Sciences, The University of Arizona, 1630 East University Blvd., Tucson, Arizona 85721, USA*

We investigate the nonlinear propagation of multiterawatt femtosecond laser pulses at 800 nm wavelength in air, under different external focusing conditions. We profile the laser beam in the vicinity of the nonlinear focus using a technique based on the dependence of the single-shot ablation threshold for gold on the angle of incidence of the laser beam on the sample. Under very tight focusing conditions (f number $\sim$15) we observe the propagation regime reminiscent of the nanosecond optical breakdown. No clear individual filaments are formed across the beam, and the estimated peak intensity surges to at least 200 TW/cm^2. As the external focusing is loosened to f number $\sim$125, we observe the transition to the multifilamentation regime. Distinct individual filaments are formed before the linear focus while the peak intensity reaches $\sim$80 TW/cm^2. Once formed, the filaments do not coalesce into a single or few superfilaments as they pass through the focus zone. Our experimental observations are supported by numerical simulations.

I. INTRODUCTION

Femtosecond laser filamentation is a self-channeling propagation regime for ultrashort, intense laser pulses in air that has numerous potential applications, ranging from remote sensing to channeling of the dielectric breakdown of air [1,2]. Since self-focusing of the laser beam in the propagation medium is an essential requirement for filamentation, the peak power of the laser pulse needs to exceed the self-focusing threshold in order for the filaments to form. In air, the self-focusing threshold power is in the range from 3 to 10 GW, depending on the duration of the laser pulse.

Since the first reports on the observation of laser filaments in air [3], air filamentation has been extensively studied in the regime when a single filament or few filaments developed within the laser beam. The scenario of laser filamentation in gases derived from those studies involves the competition between different focusing and defocusing effects that the propagating laser beam experiences: The combined focusing effects of nonlinear self-focusing and external focusing with, e.g., a lens or a concave mirror is counteracted and, in a dynamic sense, balanced by beam diffraction, nonlinear losses due to strong-field ionization of air, and defocusing on the generated electron plasma. As a result of this competition, peak laser intensity is limited by (or clamped at) a particular value on the order of 100 TW/cm^2.

The value of the clamped intensity inside the filament is too high to be measured directly [4]. Consequently, conflicting statements on its dependence on the experimental conditions, e.g., external focusing, have been reported. In [5], it has been argued that the clamped intensity is virtually independent of the external focusing, while the dependence was argued to be quite strong in [6].

The negative lensing by the plasma is often referred to as the key effect in filament stabilization and intensity clamping [2]. It is important to point out that plasma defocusing relies not only on the density of free electrons, but also on the transverse curvature of the electron density profile. Therefore, when all oxygen molecules in the air become ionized near the beam axis, the plasma profile flattens and its negative lensing ability diminishes. At the same time, nonlinear losses to ionization are also reduced because there are no neutral oxygen molecules left to ionize. In the absence of those limiting effects, the laser intensity on the beam axis is no longer clamped and can surge to very high values, until the threshold for double ionization of oxygen molecules or for single ionization of molecules with higher ionization potential, e.g., nitrogen, is reached [7]. This situation is reminiscent of the conventional optical breakdown extensively studied with nanosecond lasers under tight focusing conditions in the 1960s–1970s [8].

With the advent of multiterawatt ultrafast laser systems, new propagation phenomena that involve the generation of multiple filaments within the beam profile have emerged. When the optical power of the laser pulse is many times the critical power for self-focusing, the transverse modulation instability partitions the laser beam into multiple filaments [9],

*ppolynkin@optics.arizona.edu

which are individually regularized through the mechanism discussed above and, under certain conditions, interact with each other. The filament interaction may result in the rogue-wave phenomena [10], phase transitions in multifilamentation [11], and the coalescence of multiple filaments, individually formed on the way towards the focal plane of the optical system, into a structure termed the superfilament [12]. It has been argued that for superfilamentation to occur, the laser beam, carrying peak power many times the critical power for self-focusing, has to be relatively tightly focused with an external focusing optic.

In the original publication on superfilamentation [12], burn patterns produced by the laser beam on a photographic paper have been used for imaging the beam profile. Since photographic paper has a rather low threshold for laser damage $\lesssim 10$ TW/cm^2, this type of diagnostic provided limited means for profiling the beam. Based on numerical simulations, the conclusion was drawn that both the intensity and the plasma density significantly exceeded those in the case of a single filament formed by self-focusing of a collimated, lower-energy laser beam.

Recently, a new method for profiling intense laser beams has been suggested which is based on the dependence of the single-shot ablation threshold of common materials on the angle of incidence (AOI) of the laser beam on the sample [13]. By applying this method, slices of the beam profile, at a specific fluence level, can be straightforwardly recorded. We point out that this method profiles laser fluence, not intensity. The value of intensity is derived from the value of fluence by assuming that the temporal pulse shape does not appreciably change on propagation. It has been shown by numerical simulations that short temporal spikes can develop within the pulse as it propagates through the filamentation zone [14]. Therefore, the application of the ablation-based method [13] for profiling intensity yields the intensity of an equivalent Gaussian pulse with the duration and energy equal to those of the incident pulse.

The range of fluence that can be reliably measured using the ablation-based method with a first-surface gold mirror as a sample is from 1 J/cm^2 to $\sim$10 J/cm^2. For a 50-fs-long laser pulse, that corresponds to the intensity range from about 20 TW/cm^2 to about 200 TW/cm^2. In [15], this method has been applied to profiling fluence in a single filament under different external focusing conditions. In agreement with earlier reports, it has been shown that the intensity in a single laser filament, produced by a 50-fs-long laser pulse at 800 nm wavelength, is clamped, but the value of the clamping intensity strongly depends on external focusing. For very loose focusing with f number over 500, the peak clamped intensity is $\sim$55 TW/cm^2, while for tighter focusing, with f number approaching 100, the peak clamped intensity can be as high as 200 TW/cm^2. The intensity is clamped with respect to the input pulse energy, not with respect to the conditions of external beam focusing.

In this paper, we apply the ablation-based method to profiling multiterawatt laser beams propagating in air under different focusing conditions. We consider two cases. In the first case, we use very tight focusing with f number of about 15. We show that the peak intensity in this case exceeds 200 TW/cm^2, which is the upper limit of our measurement technique. It is in agreement with the evaluation obtained

from numerical simulations under similar focusing conditions [7]. As our numerical simulation shows, a complete single ionization of all oxygen molecules in the air is reached in this case. The plasma profile near the beam axis flattens and its ability to produce negative lensing of the beam is diminished, allowing the intensity to surge to very high values. This interaction regime is reminiscent of the familiar nanosecond optical breakdown.

The second propagation regime we investigate is under the conditions very similar to those used in the report on superfilamentation [12]. Differently from [12], we can experimentally profile the beam at several intensity levels and obtain quantitative data for the formation and interaction of multiple filaments, at different longitudinal positions, as the beam propagates through the focal plane of the focusing optic. As we show, the peak intensity reaches 80 TW/cm^2, which is consistent with the estimate based on numerical simulations in [12]. We show that multiple filaments, formed before the focal region of the lens, travel through the focal plane without coalescing together into a single or few superfilaments. These conclusions are supported by numerical simulations.

Note that measurements of the density of laser-generated plasma channels in air, under the conditions similar to those used in our present work, have been reported in [16]. The ultrafast shadowgraphy and interferometry techniques, used in [16], yield two-dimensional images of the refractive index profile, averaged along the propagation path of the probe beam. Several individual filaments that may accidentally line up in the plane of propagation of the probe beam will be perceived by the interferometric measurement as a single, denser filament. Furthermore, extracting the values of the optical intensity from the measured values of plasma density relies on the calculation using ionization rates of air molecules, which are not precisely known. Our measurement approach is free from these limitations and directly yields the true fluence profile of an arbitrary and not necessarily axially symmetric laser beam. The intensity profile is then calculated based on the fluence data under the fixed pulse-shape approximation.

II. RESULTS AND DISCUSSION

A. Experimental setup

Our experiments have been conducted using the JETI-40 laser system at the Institute of Optics and Quantum Electronics, the Friedrich-Schiller University in Jena, Germany. The laser delivers optical pulses with duration of about 40 fs, at 10-Hz pulse repetition rate. In our experiments, the energy of the individual laser pulses is in the range from 100 to 120 mJ. An electro-optic shutter incorporated into the laser system is used for single-shot experiments.

The technique that we use for the measurements of the fluence profile of the laser beam in the vicinity of the ionization zone is discussed in detail in [13,15]. In brief, the single-shot ablation threshold of the gold surface for an S-polarized laser beam steadily grows, in a tabulated fashion, from 1.0 J/cm^2 to 8.6 J/cm^2, as AOI of the laser beam on the sample is increased from zero degrees (normal incidence) to 70°. The corresponding range of peak intensity of the laser pulse, assuming 40 fs FWHM temporal pulse shape, is from 80 TW/cm^2 to

200 TW/cm^2. To profile the laser beam, at a particular location along the propagation path we produce single-shot ablations of a 100-nm-thick, unprotected gold coating on a standard silicon wafer. The resulting ablation marks are photographed and scaled, by the factor cos(AOI), along the direction of the sample tilt. The outer boundary of the burn mark shows the line-out of the beam, at a particular fluence level, which is equal to the ablation threshold fluence for the particular AOI that the ablation has been produced at.

We point out that only the edge of the burn pattern bears quantitative information about the local fluence of the beam. The internal parts of the ablation marks correspond to the locations within the beam, where the beam fluence exceeds the ablation threshold fluence by some unknown value. The morphology of these internal portions of the burn patterns can be affected by the interaction of the sample with the plasma that results from the strong-field ionization of air molecules. These issues are discussed in detail in [15].

B. Numerical model

Numerical simulations of the propagation of multiterawatt laser pulses under tight focusing are challenging because of the very high levels of ionization and the associated abrupt beam dynamics. We resort to the treatment based on the unidirectional propagator, including nonparaxial diffraction and assuming an invariant temporal profile of the pulse along propagation. Both in air and in water, this approach faithfully reproduces experimental beam patterns in multifilamentation of femtosecond laser pulses with peak power significantly above critical [7,12,17]. Throughout the simulations, we use the 8th-power super-Gaussian input beam profile with a diameter of 55 mm and a pulse duration of 40 fs FWHM. 20% intensity noise is added to the input beam to mimic the realistic experimental beam profile. Similar to the treatment used in [7], ionization of both oxygen and nitrogen is accounted for, together with the two corresponding nonlinear absorption channels. Our numerical model and the propagation code are discussed in detail in [18].

C. Tight focusing—femtosecond optical breakdown

We first discuss the case of very tight focusing, with the focusing f number of about 15. In the experiment, the 6-cm-diameter, flat-top laser beam is sharply focused by a lens with a focal length of 90 cm. The pulse energy is 100 mJ.

The single-shot ablation patterns produced by the laser beam on the gold-coated silicon wafers at different AOIs of the laser beam on the sample are imaged under an optical microscope and digitally photographed. The images are subsequently digitally shrunk, by the factor cos(AOI), along the direction of the sample tilt. The resulting patterns are shown in Fig. 1. Here, the samples are tilted, by various AOIs, around the vertical axis and shrunk horizontally. The laser beam is propagating into the plane of the shown images.

The boundaries of the shown patterns correspond to the positions within the beam, where the local intensity is exactly at the level of the ablation threshold, for the specific AOI. The data are grouped into columns corresponding to three values of the AOI: 0°, 60°, and 70°. Assuming a 40-fs-long Gaussian
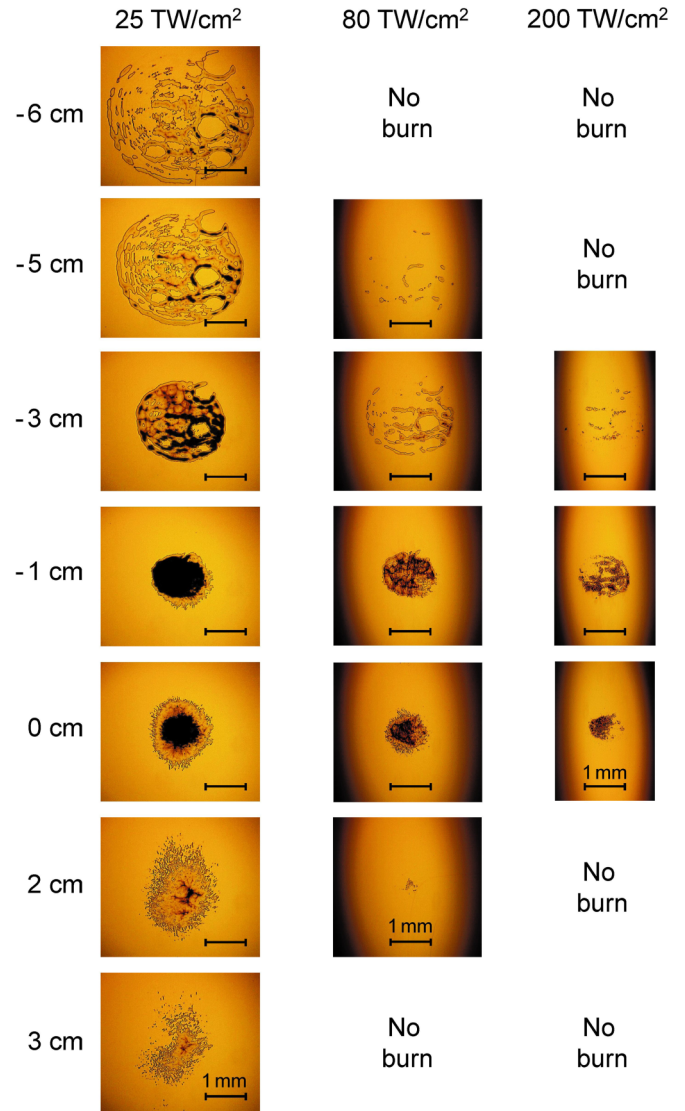

FIG. 1. Experimental beam profiles at different intensity levels and at different longitudinal positions relative to the linear focus of the lens for the case of very tight beam focusing with an f number of about 15. The energy of the 40-fs-long input laser pulse is 100 mJ. No clear individual filaments are formed on propagation. Instead, the intensity relatively uniformly surges to at least 200 TW/cm^2.

pulse, the values of ablation threshold intensity for gold, corresponding to these values of the AOI, are 80 TW/cm^2, 80 TW/cm^2, and 200 TW/cm^2 [13], as indicated at the top of the columns. The longitudinal coordinates shown to the left are relative to the geometrical focal plane of the focusing lens.

It is evident from these images that the geometrical focusing of the beam is the dominant effect that drives the propagation dynamics. The beam focuses as a whole, without forming clear individual filaments. The peak intensity on the beam axis surges to at least 200 TW/cm^2, which is the upper limit of the intensity range that can be reliably measured with our ablation-based method.

The results of the corresponding numerical simulations are shown in Fig. 2. The computed beam patterns before the geometrical focus qualitatively agree with those observed in
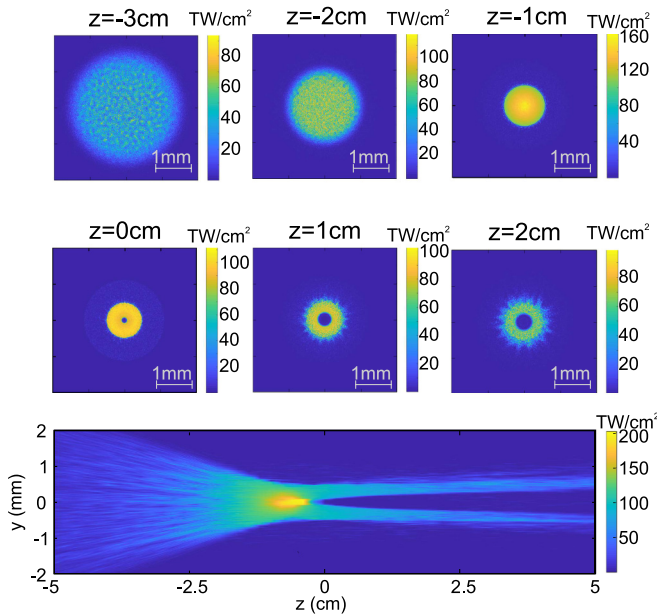
FIG. 2. Results of numerical simulations for the case with very tight external beam focusing, corresponding to the experimental results shown in Fig. 1. The ring intensity structure formed after the linear focus is the artifact of the constant-temporal-envelope approximation used in the numerical model, as discussed in the text.

FIG. 3. Same as in Fig. 1, but with external beam focusing loosened to the f number of about 125 and the laser-pulse energy of 120 mJ. The beam patterns show the formation of multiple individual filaments with a diameter of $\sim 100\ \mu$m and peak intensity reaching 80 TW/cm^2. As these filaments travel through the focus zone, an intensity pedestal builds up to the relatively high level of about 40 TW/cm^2, but the individual filaments on top of the pedestal do not coalesce into one or few superfilaments.

the experiment, although the highest intensity at the focus is somewhat lower than what is experimentally measured. No individual filaments are formed on propagation towards the geometrical focal plane. After the focus, the simulation shows the formation of a conically diverging intensity ring that is not observed in the experiment. This discrepancy may be partly due to the use of the 8th-power super-Gaussian input beam profile assumed in our numerical model; such initial conditions are known to promote the formation of an intensity ring [19]. In addition, due to the frozen pulse profile used in the simulation, the model overestimates the nonlinear losses and plasma defocusing of the leading temporal edge of the pulse, which, in reality, is much less affected by those effects than the trailing edge. Differently from the simulation, in the experiment, the intact leading edge of the pulse populates the far field propagating near the beam axis, filling the hole in the intensity ring produced by the trailing edge.

Before the focus, both experiment and simulation show that the lens rapidly builds up the intensity pedestal to the level sufficient for driving significant ionization of air molecules. Ionization losses and plasma defocusing prevent the transverse modulation instability from forming distinguishable filaments.

Near the focus, the simulation shows a complete single ionization of oxygen and ionization of $\sim 9\%$ nitrogen. As discussed above, the plasma, produced through ionization of oxygen, loses its negative lensing ability because its transverse intensity profile flattens. Following complete single ionization of oxygen, nitrogen starts to be ionized rapidly. Nitrogen ionization becomes the nonlinear mechanism that limits the maximum laser intensity at the focus.

We point out that this case presents an example of extreme nonlinear interaction and propagation. The apparent discrepancy between experiment and simulation is not unexpected,
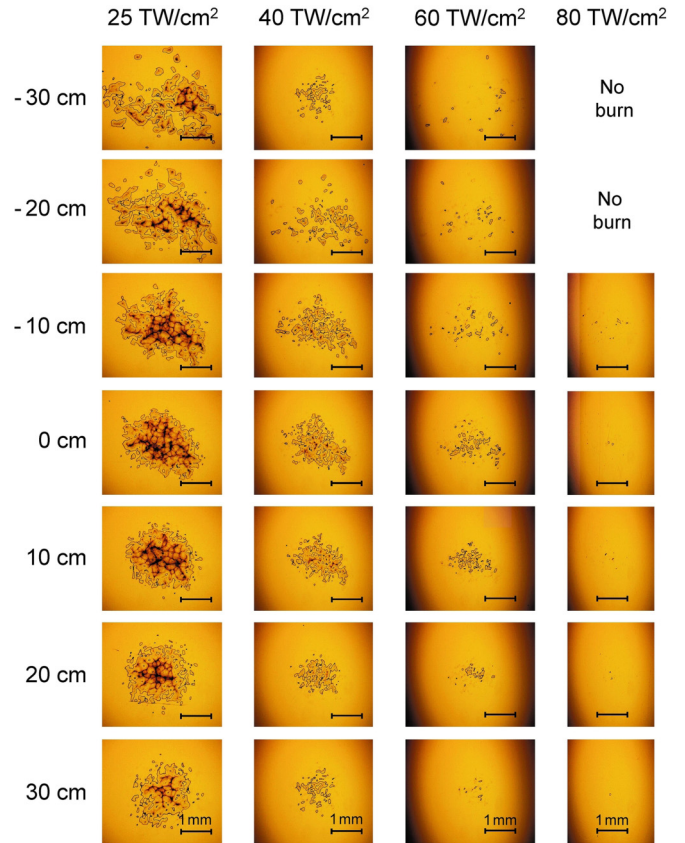
given the approximations made in order to make the simulation computationally feasible and the limited accuracy to which the relevant material parameters are known.

D. Weaker focusing—multifilamentation

We now discuss the results for the case of moderately strong focusing, when the same 6-cm-diameter laser beam is focused by a focusing lens with a focal length of 7.5 m, corresponding to an f number of about 125. The pulse energy in this case is 120 mJ. These conditions are very similar to those used in the original paper on superfilamentation [12]. Here, the beam profiling experiments using the ablation-based method are performed with values of the angle of incidence of the laser beam on the gold surface of 0°, 45°, 54°, and 60°. The corresponding values of ablation threshold intensity for the gold surface, assuming a 40-fs Gaussian pulse, are 25 TW/cm^2, 40 TW/cm^2, 60 TW/cm^2, and 80 TW/cm^2, respectively [13].

The images of single-shot ablation patterns produced by the laser beam on the gold-coated wafer samples are shown in Fig. 3. As in the case of tight focusing, shown in Figure 1, the wafer samples are tilted around the vertical axis and their microscope images are shrunk horizontally. The laser pulse
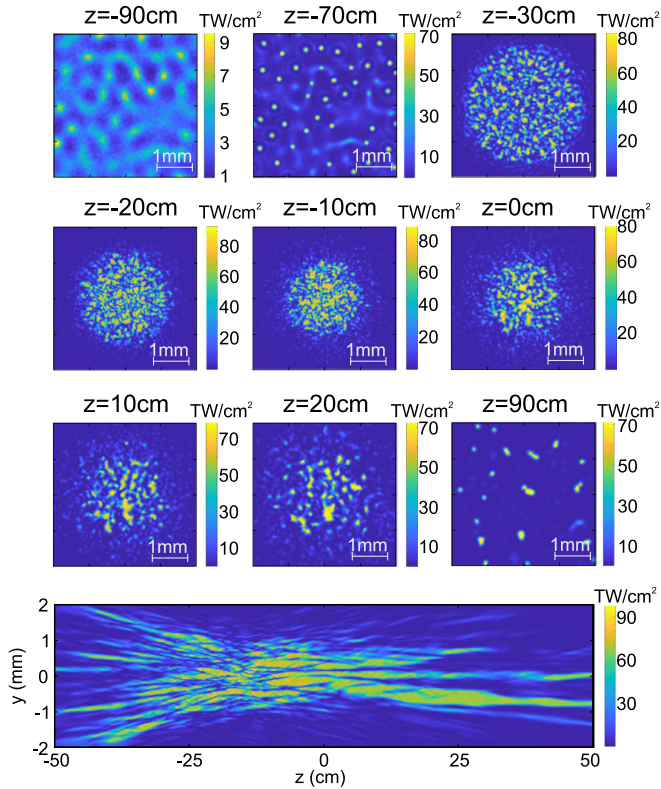
FIG. 4. Results of numerical simulations for the case with moderately strong focusing, shown in Fig. 3. Computed beam-intensity patterns are in semiquantitative agreement with those experimentally measured.

propagates into the plane of the shown images. The results of the accompanying numerical simulations are shown in Fig. 4.

In this case, experiments and simulations agree quite well. The major result that can be derived from these data is that the individual filaments that are formed before the nonlinear focus (intensity level above $\sim$60 TW/cm^2), pass through the focus zone without merging into a single or several superfilaments. The modulation instability starts fragmenting the beam into filaments long before the geometrical focus, where the intensity is below 10 TW/cm^2. Further down the propagation path, external focusing builds up the intensity pedestal to the level $\sim$40 TW/cm^2 over the area with a transverse size on the order of 2 mm. The maximum peak intensity inside individual filaments is on the order of 80 TW/cm^2, which is similar to the

estimate based on the numerical simulation reported in [12]. As evidenced by the experimental data, the beam pattern is more compact after passing through the linear focus than before the focus, which is the signature of nonlinear self-channeling. The simulation shows ionization of oxygen and nitrogen molecules on the levels of $\sim$10% and 0.1%, respectively.

As pointed out above, we have not observed the propagation regime, in which the individual filaments, already formed on the way towards the focal plane of the focusing optic, coalesced into a single or several superfilaments, as may be inferred from the title and discussion in [12]. However, based on our observations, we cannot definitively conclude that the coalescence of filaments cannot occur in principle. To draw a conclusion on such a possibility, quantitative definitions of filament coalescence and superfilamentation would need to be formulated, and a detailed study, covering focusing conditions in between the two particular cases we considered, would be necessary.

III. SUMMARY

To summarize, we have measured the intensity profiles of multiterawatt femtosecond laser beams propagating in air under two distinctly different focusing conditions. In the case of very tight focusing, the propagation regime reminiscent of the nanosecond optical breakdown was observed. Strong external focusing dominated the propagation dynamics. No clear individual filaments were observed, and the beam intensity in the focal plane surged above 200 TW/cm^2. Numerical simulation showed a complete single ionization of oxygen molecules in the vicinity of the focus. In the case of moderately strong focusing, multiple individual filaments were formed well before the focus and propagated through the focal zone without coalescing into a single or few superfilaments. This conclusion is supported by the accompanying numerical simulations.

[1] A. Couairon and A. Mysyrowicz, Phys. Rep. **441**, 47 (2007).

[2] S. L. Chin, *Femtosecond Laser Filamentation* (Springer, New York, 2010).

[3] A. Braun, G. Korn, X. Liu, D. Du, J. Squier, and G. Mourou, Opt. Lett. **20**, 73 (1995).

[4] D. G. Papazoglou and S. Tzortzakis, Appl. Phys. Lett. **93**, 041120 (2008).

[5] O. G. Kosareva, W. Liu, N. A. Panov, J. Bernhardt, Z. Ji, M. Sharifi, R. Li, Z. Xu, J. Liu, Z. Wang, J. Ju, X. Lu, Y. Jiang, Y. Leng, X. Liang, V. P. Kandidov, and S. L. Chin, Laser Phys. **19**, 1776 (2009).

[6] F. Théberge, W. Liu, P. Tr. Simard, A. Becker, and S. L. Chin, Phys. Rev. E **74**, 036406 (2006).

[7] P. P. Kiran, S. Bagchi, S. R. Krishnan, C. L. Arnold, G. R. Kumar, and A. Couairon, Phys. Rev. A **82**, 013805 (2010).

[8] *Principles of Laser Plasmas*, edited by G. Bekefi (Wiley, New York, 1976).

[9] S. Skupin, L. Bergé, U. Peschel, F. Lederer, G. Méjean, J. Yu, J. Kasparian, E. Salmon, J.-P. Wolf, M. Rodriguez, L. Wöste, R. Bourayou, and R. Sauerbrey, Phys. Rev. E **70**, 046602 (2004).

[10] S. Birkholz, E. T. J. Nibbering, C. Brée, S. Skupin, A. Demircan, G. Genty, and G. Steinmeyer, Phys. Rev. Lett. **111**, 243903 (2013).

[11] D. Mongin, E. Schubert, N. Berti, J. Kasparian, and J.-P. Wolf, Phys. Rev. Lett. **118**, 133902 (2017).

[12] G. Point, Y. Brelet, A. Houard, V. Jukna, C. Milián, J. Carbonnel, Y. Liu, A. Couairon, and A. Mysyrowicz, Phys. Rev. Lett. **112**, 223902 (2014).

[13] X.-L. Liu, W. Cheng, M. Petrarca, and P. Polynkin, Appl. Phys. Lett. **109**, 161604 (2016).

[14] M. B. Gaarde and A. Couairon, Phys. Rev. Lett. **103**, 043901 (2009).

[15] X.-L. Liu, W. Cheng, M. Petrarca, and P. Polynkin, Opt. Lett. **41**, 4751 (2016).

[16] X.-L. Liu, X. Lu, X. Liu, T.-T. Xi, F. Liu, J.-L. Ma, and J. Zhang, Opt. Express **18**, 26007 (2010).

[17] V. Jukna, A. Jarnac, C. Milián, Y. Brelet, J. Carbonnel, Y.-B. André, R. Guillermin, J.-P. Sessarego, D. Fattaccioli, A. Mysyrowicz, A. Couairon, and A. Houard, Phys. Rev. E **93**, 063106 (2016).

[18] A. Couairon, E. Brambilla, T. Corti, D. Majus, O. de J. Ramírez-Góngora, and M. Kolesik, Eur. Phys. J.: Spec. Top. **199**, 5 (2011).

[19] T. D. Grow, A. A. Ishaaya, L. T. Vuong, A. L. Gaeta, N. Gavish, and G. Fibich, Opt. Express **14**, 5468 (2006).